

1 (SUPPORTING INFORMATION)

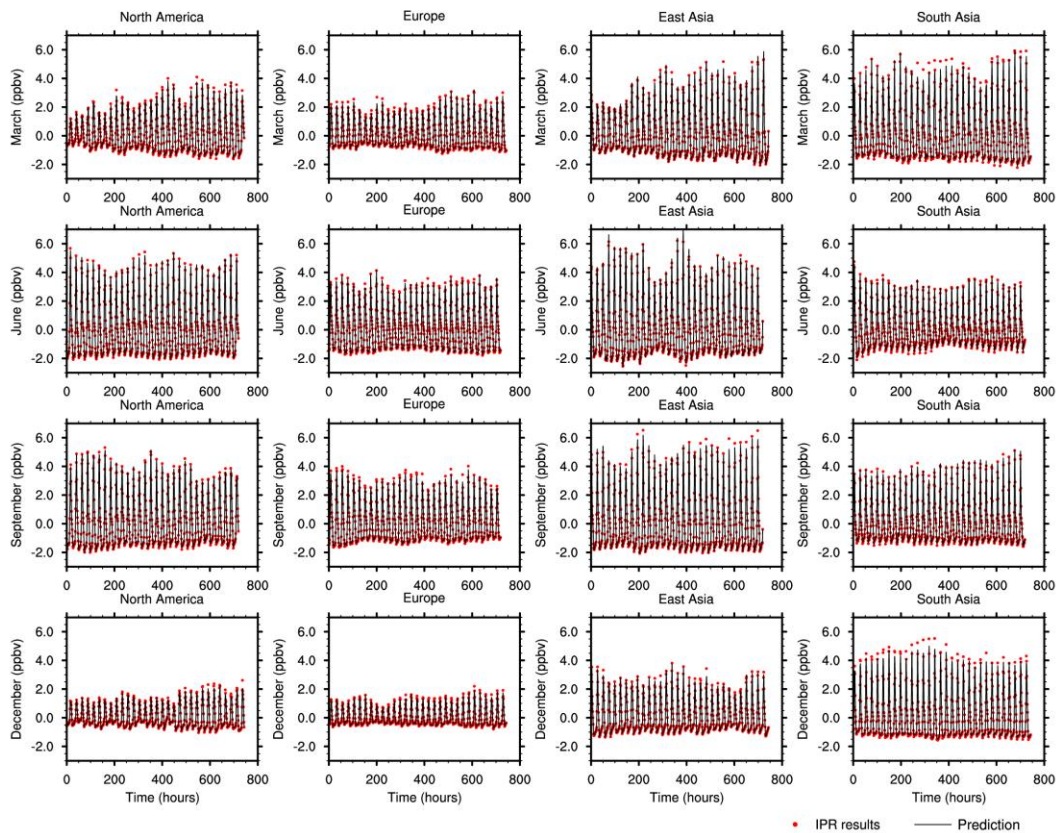
2 Response of Global Surface Ozone Distribution to  
3 Northern Hemispheric Sea Surface Temperature Changes:  
4 Implication for Long-Range Transport  
5

6 Kan Yi<sup>1</sup>, Junfeng Liu<sup>1</sup>, George Ban-Weiss<sup>2</sup>, Jiachen Zhang<sup>2</sup>,  
7 Wei Tao<sup>1</sup>, Shu Tao<sup>1</sup>  
8

9 [1] Laboratory for Earth Surface Processes, College of Urban and Environmental  
10 Sciences, Peking University, Beijing, China  
11

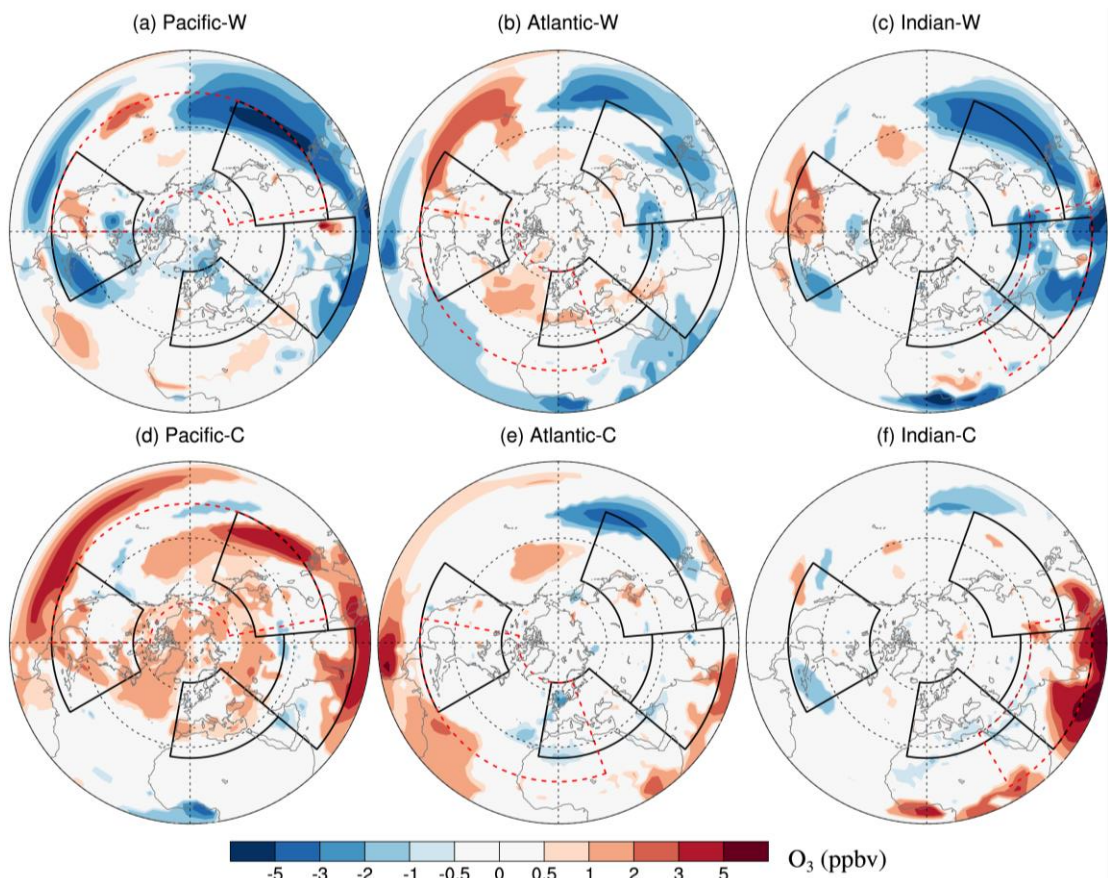
12 [2] Sonny Astani Department of Civil and Environmental Engineering, University of  
13 Southern California, U.S.A.  
14

15 Correspondence to: Junfeng Liu (E-mail: [jfliu@pku.edu.cn](mailto:jfliu@pku.edu.cn))  
16  
17



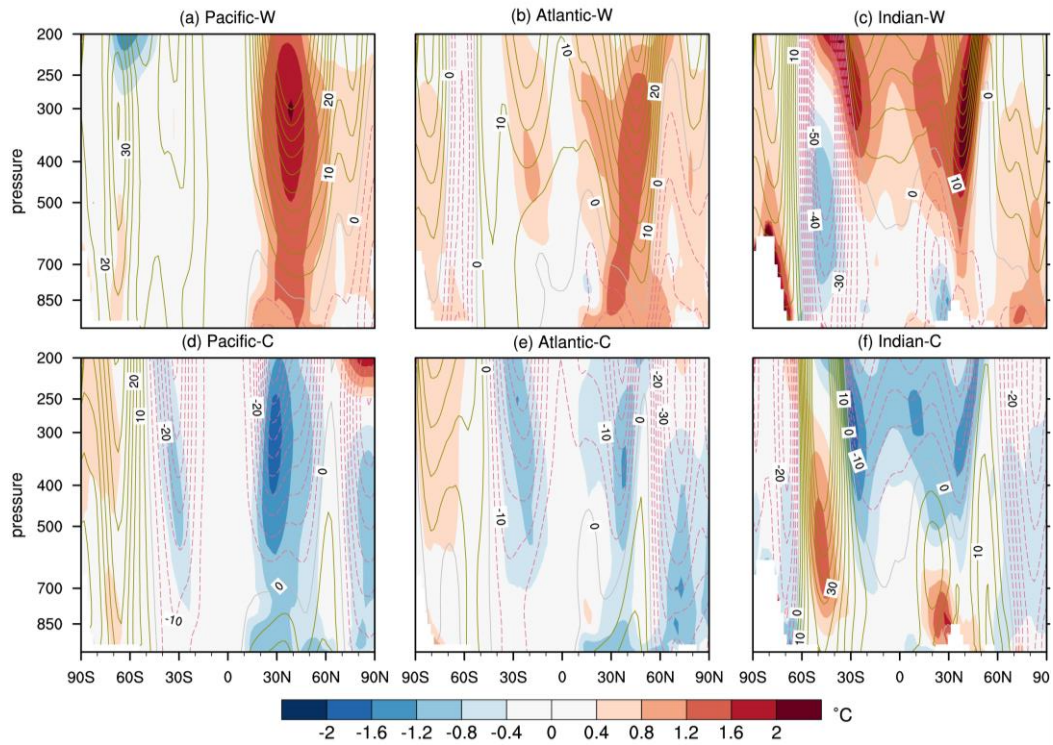
18 **Figure S1.** Hourly time-series of predicted O<sub>3</sub> changes (black lines) and the sum of IPR  
19 results (red dots) averaged over four major regions of interest (i.e., America (15°N–  
20 55°N; 60°W–125°W), Europe (25°N–65°N; 10°W–50°E), East Asia (15°N–50°N;  
21 100°E–130°E), and South Asia (10°N–25°N; 70°E–90°E)).

22 95°E–160 °E) and South Asia (5 °N–35 °N; 50 °E–95°E)) during the March (first row),  
 23 June (second row), September (third row) and December (last row) of random modeling  
 24 years in CTRL.  
 25



26  
 27 **Figure S2.** Changes in the wintertime (December-February) surface ozone  
 28 concentrations (ppbv) in the Northern Hemisphere induced by 1°C warming (top) and  
 29 1°C cooling (bottom) in the North Pacific Ocean (left), North Atlantic Ocean (center),  
 30 and North Indian Ocean (right) relative to CTRL. Four major regions of interest (i.e.,  
 31 NA (15°N–55 °N; 60°W–125°W), EU (25°N–65 °N; 10°W–50 °E), EA (15 °N–50 °N;  
 32 95°E–160 °E) and SA (5 °N–35 °N; 50 °E–95°E)) are marked with black polygons. Red  
 33 dashed lines mark the regions where the SST has been changed. Only results significant  
 34 at the 0.1 level evaluated with a Student t-test are depicted.

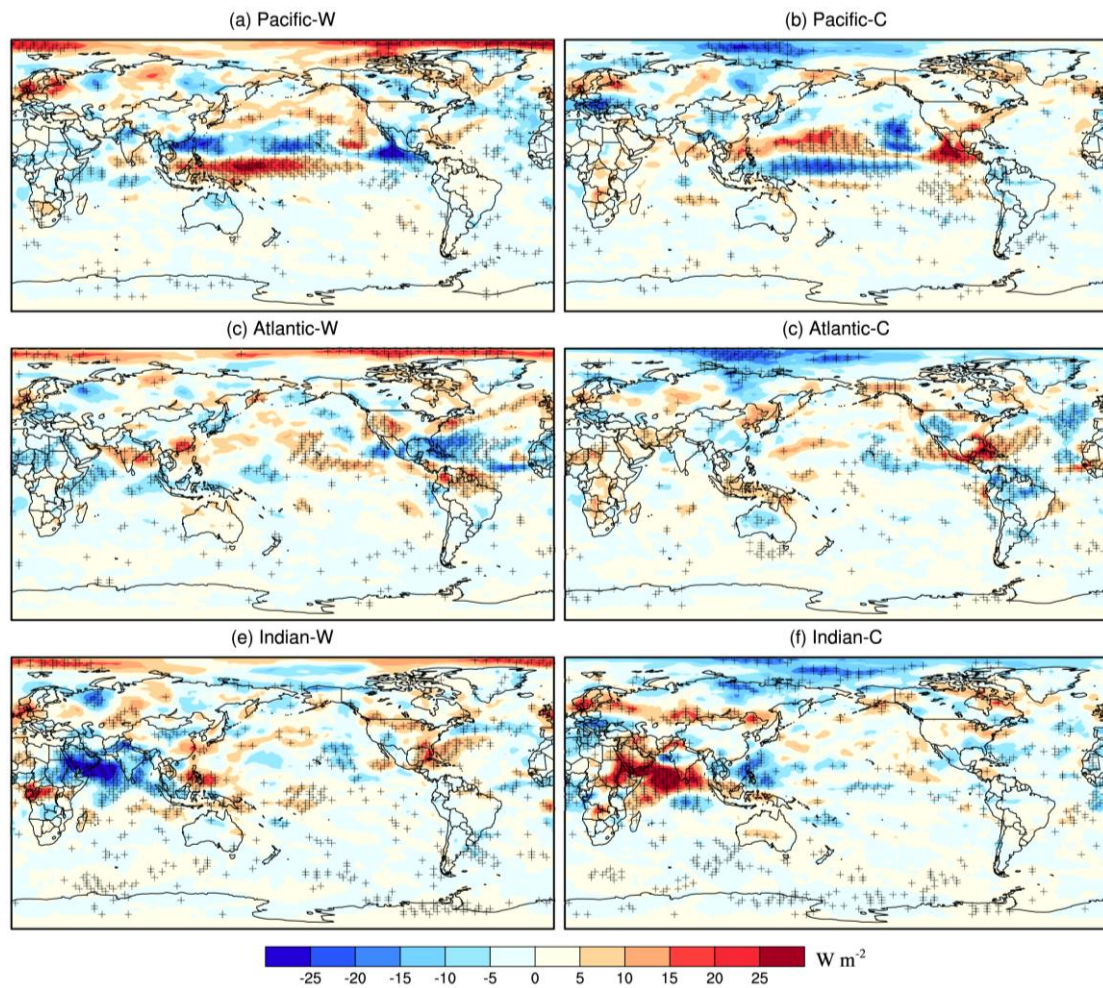
35



36

37 **Figure S3.** Vertical and latitudinal distributions of air temperature differences (color  
 38 contours, °C ) and geopotential height anomalies (contours, m) longitude averaged  
 39 from 150°W-180°W for (a) Pacific\_W and (d) Pacific\_C, 50°E-80°E for (b) Atlantic\_W  
 40 and (e)Atlantic\_C, and 20°W-40°W for (c) Indian\_W and (f) Indain\_C, relative to  
 41 CTRL.

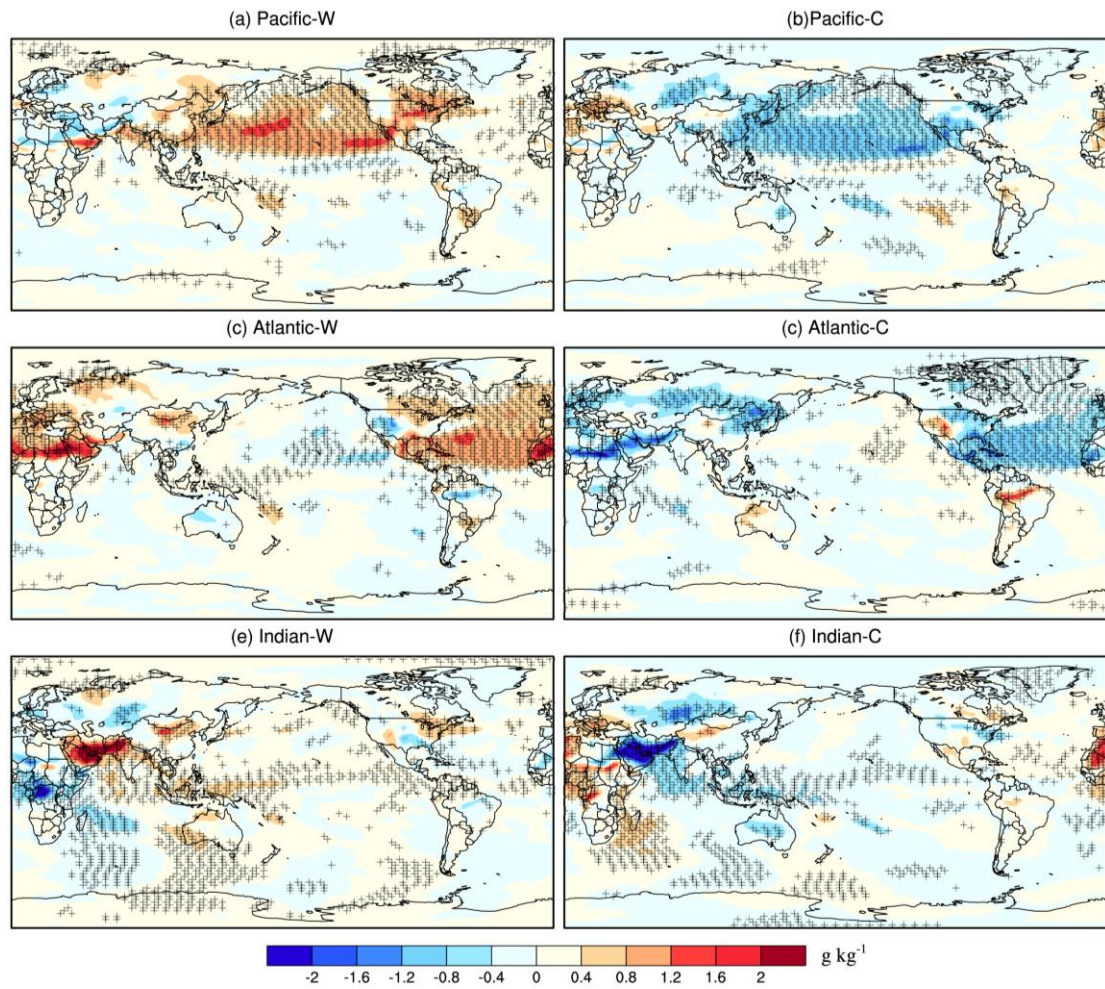
42



43

44 **Figure S4.** Perturbations of surface solar radiations ( $\text{W m}^{-2}$ ) relative to CTRL for (a)  
 45 Pacific-W, (b) Pacific-C, (c) Atlantic-W, (d) Atlantic-C, (e) Indian-W and (f) Indian-C  
 46 in the summertime (June-August). The + symbols denote areas where results are  
 47 significant at the 0.05 level evaluated with a Student t-test.

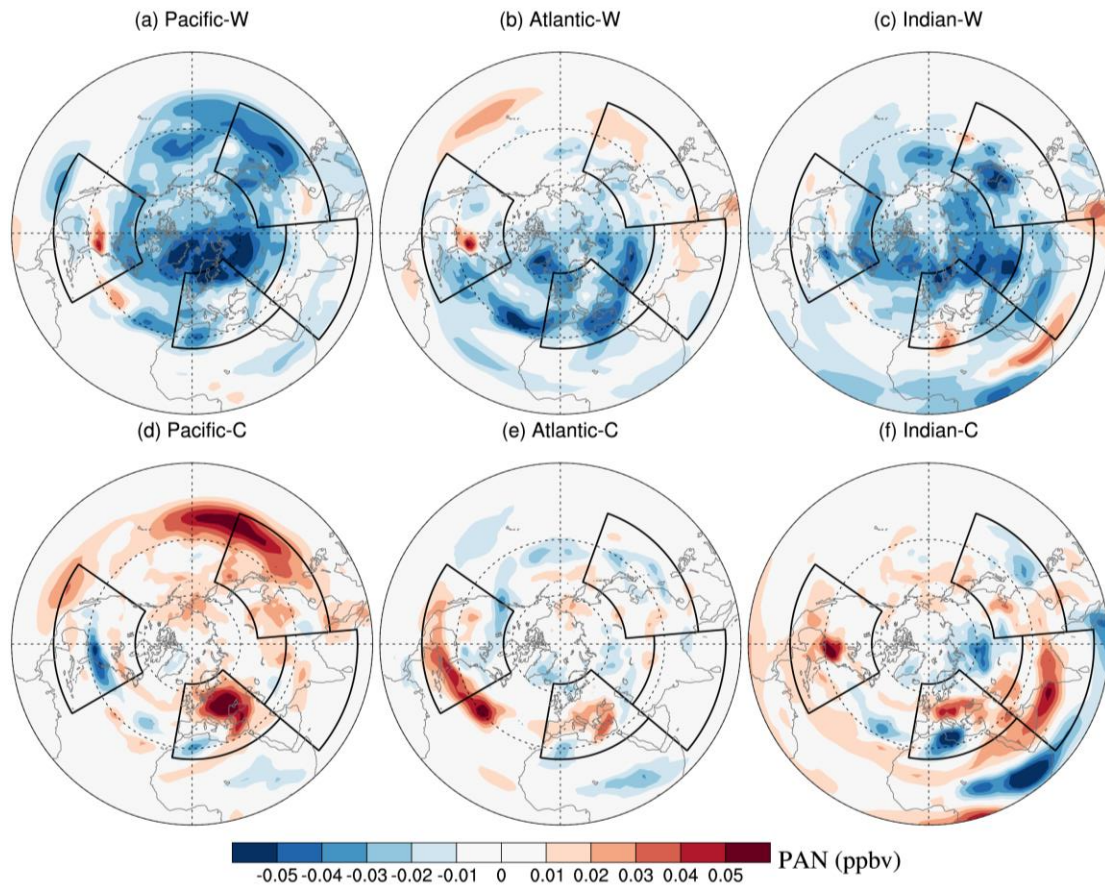
48



49

50 **Figure S5.** Same as Figure S5 but for surface specific humidity ( $\text{g kg}^{-1}$ ).

51



52

53 **Figure S6.** Changes in PAN concentrations (ppbv) at 500 hPa in the Northern  
 54 Hemisphere for (a) Pacific-W, (b) Atlantic-W, (c) Indian-W, (d) Pacific-C, (e) Atlantic-  
 55 C and (f) Indian-C relative to CTRL in the summertime (June-August). Four major  
 56 regions of interest (i.e., NA (15°N–55 °N; 60°W–125°W), EU (25°N–65 °N;10°W-  
 57 50 °E), EA (15 °N–50 °N; 95°E–160 °E) and SA (5 °N–35 °N; 50 °E–95°E)) are marked  
 58 with black polygons.

59